Gas to particle partitioning of organic compounds in ADCHEM

This document contains an updated version chapter 2.2.2 and 2.4 in the model description paper Roldin et al. (2010). This updated model description will be included in the final paper.

2.2.2 Condensation and evaporation

ADCHEM considers condensation or evaporation of sulfuric acid, ammonia, nitric acid, hydrochloric acid and oxidation products of different organic compounds. Figure 2 illustrates the structure of the condensation/evaporation algorithm used in ADCHEM. The condensation and evaporation is solved by first calculating the single particle molar condensation growth rate of each compound, for each size bin separately (Eq. (2)). If considering uncoupled condensation of acids and ammonia the analytic prediction of condensation (APC) scheme and predictor of non-equilibrium growth (PNG) scheme developed and described in detail by Jacobson (1997, 2005a) are used, while if treating the condensation of acids and ammonia as a coupled process the method first proposed by Wexler and Seinfeld (1990) and later applied by e.g. Zhang and Wexler (2008) is used. The coupled condensation growth rate of NH_3 and HX (mol/s) is given by Eq. (3), where X denotes either Cl or NO_3. The total NH_3 condensation growth rate (I_{NH3}) is then given by the sum of the HCl, HNO_3 and 2 times the S(VI) condensation growth rates ($I_{NH3}=2I_{S(VI)}+I_{HNO3}+I_{HCl}$). Both methods are mass and number conserving when combined with either the full-stationary, full-moving or moving-center structure. The APC scheme is used for condensation/evaporation of organics, sulfuric acid and for HCl and HNO_3 if they form solid salts with ammonium, while for dissolution of HCl and HNO_3 into the particle water phase, the PNG scheme is used instead (Jacobson, 2005a). In this scheme dissolution of ammonia is treated as an equilibrium process solved after the diffusion limited condensation/evaporation of HNO_3, HCl and H_2SO_4. Treating the dissolution of NH_3 as an equilibrium process enables the model to take long time steps (minutes) when solving the condensation/evaporation process (Jacobson, 2005a). This method can easily be modified to treat the ammonia dissolution as a dynamic process. However, this requires that the time step is decreased drastically to prevent oscillatory solutions.

$$I_i = \frac{dc_{p,i}}{dt} = \frac{2D_i D_p}{RT} f_i(Kn_i, \alpha_i)(p_{i\infty} - p_{i_s})$$
$$f_i(Kn_i, \alpha_i) = \frac{0.75\alpha_i(1 - Kn_i)}{Kn_i^2 + Kn_i + 0.283Kn_i\alpha_i + 0.75\alpha_i} \quad (2)$$

$$I_{HX} = \frac{\pi D_p \overline{D}\overline{C}}{f_{NH_3}} \left(1 - \sqrt{1 - \frac{4 f_{NH_3}{}^2 \left(C_{NH_3,\infty} C_{HX,\infty} - C_{NH_3,s} C_{HX,s} \right)}{\overline{C}^2}} \right)$$
$$\overline{D} = \sqrt{D_{NH_3} D_{HX}} \quad (3)$$
$$\overline{C} = (D_{NH_3} C_{NH_3} + D_{HX} C_{NH_3}) \big/ \overline{D}$$

In Eq. (2) and (3), I_i is the contributions of species i to the mole and diameter growth rates, respectively, f_i is the Fuchs-Sutugin correction factor in the transition region, C_i is the gas phase concentration of species i in moles m^{-3} air, D_p is the particle diameter, t is the time, T is the temperature, R is the ideal gas constant, Kn_i is the non-dimensional Knudsen number, α_i is the mass accommodation coefficient, $p_{i,\infty}$ is the partial pressure and $p_{i,s}$ is the saturation vapor pressure. The mass accommodation coefficients for HNO_3, NH_3, H_2SO_4, HCl, SO_2, H_2O_2 and organic vapors were set to 0.2, 0.1, 1.0, 0.2, 0.11, 0.23 and 0.1 respectively. For the inorganic compounds these numbers are within the range of values tabulated in Sander et al. (2006) over liquid water at temperatures between 260 and 300 K. As a sensitivity test one simulation was also performed with unity mass accommodation coefficients. Usually it is assumed that the saturation vapor pressure of sulfuric acid is zero (Korhonen, 2004a and Pirjola and Kulmala, 1998). The saturation vapor concentrations of ammonia, nitric acid and hydrochloride acid and the equilibrium concentration of sulfuric acid and hydrogen peroxide are calculated using a thermodynamic model described in Sect. 2.2.8.

The VBS approach (Donahue et al., 2006) and the two-product model (Odum et al., 1996), build on the partitioning theory from Pankow (1994), which describes the equilibrium gas and particle partitioning of organic vapors (see Sect. 2.4). When using the VBS method ADCHEM considers the kinetic (diffusion limited) condensation/evaporation of 110 different organic compounds, while when using the two-product model approach the number of condensable organic compounds is 37. Both methods take into account the Kelvin effect which gives a particle size dependent partitioning of the different condensable organic compounds, with larger fraction of

low volatile compounds found on the smaller particle sizes and a larger fraction of more volatile compounds found on the larger particle sizes. This kinetic and particle size dependent condensation/evaporation requires that ADCHEM keep track of all the different organic compounds in each particle size bin, which is computationally expensive, especially for the coagulation algorithm.

The VBS method gives the amount of SOA formed as a function of the exposure to the oxidation agents (e.g. OH) (Jimenez et al., 2009). This way the SOA formation in the model can be treated as a dynamic process that evolves over time, taking into account that the SOA production depends on the initial volatility of the emissions, the oxidation state of the emissions, the oxidation agent concentration, the time of ageing (exposure time) and meteorological conditions (temperature).

In the 2-product model the SOA formation also depends on the time of ageing and concentration of oxidation agents, but it is only the initial oxidation step which determines the properties of the final products, which is represented by two surrogate compounds formed from each reaction between a SOA-precursor and an oxidation agent. Therefore the 2-product model cannot take into account the fact that more volatile compounds generally need longer time (several oxidation steps) of ageing before they are incorporated into the aerosol phase than less volatile compounds.

2.4 Species specific SOA yields and source specific 2D-VBS

The secondary organic aerosol formation in ADCHEM can either be modeled with the traditional two product model approach (Odum et al., 1996), or the recently proposed VBS approach (Donahue et al., 2006 and Robinson et al., 2007). One advantage with the two product model used in ADCHEM is that it models the SOA formation from specific organic compounds, formed from oxidation products of a few well characterized compounds known to form SOA (e.g. oxidation products of monoterpenes, isoprene, benzene, toluene and xylene). However the SOA formation in the atmosphere is complex and involves thousands of unknown compounds (Donahue et al., 2006).

The VBS scheme lumps all organic species into different bins according to their volatility (given by their saturation concentration (C^*), at 298 K) (Robinson et al., 2007). This method thereby

generally loses the information of the chemical reactions in where individual organic compounds are involved in, but is designed to be able to predict realistic SOA formation rates found in the atmosphere using a model with relatively low complexity and only a few model parameters.

Recently, Jimenez et al. (2009) developed a 2D-VBS method which apart from classifying the organic compounds according to their volatility also includes a second dimension, oxygen to carbon ratio (O:C-ratio). This 2D-VBS method is implemented in ADCHEM, with slightly different assumptions which will be described below.

2.4.1 Kinetic SOA formation with the two-product model

According to the two-product model developed by Odum et al. (1996) the aerosol yield *(Y)* can be parameterized as a function of the aerosol organic mass according to Eq. (10).

$$Y = M_o \left(\frac{\alpha_1 K_{om,1}}{1 + K_{om,1} M_o} + \frac{\alpha_2 K_{om,2}}{1 + K_{om,2} M_o} \right) \tag{10}$$

M_o is the organic particle mass in µg m^{-3}, $K_{om,i}$ is the partitioning coefficient of product *i*, α_i is the mass based stochiometric yield of product *i*. Values of α_i and $K_{om,i}$ from Griffin et al. (1999), Svendby et al. (2008), Henze and Seinfeld (2006) and Ng et al. (2007) are given in Table S2 in the online supplementary material, for all organic oxidation products forming secondary organic aerosol in the model. $K_{om,1}$ and $K_{om,2}$ describes the volatility of two surrogate oxidation products which represent all the reaction products from an oxidation agent and a SOA precursor. Equation 11 gives the mass fraction $(F_{p,i})$ of the oxidation product *i* which at equilibrium will partition into the particle phase. If the gas and particle phase concentrations of the oxidation product *i* deviate from this equilibrium, the diffusion limited mass transfer (condensation or evaporation) drives the concentrations closer toward this equilibrium state (see Sect. 2.2.2).

$$F_{p,i} = \frac{M_o K_{om,i}}{1 + K_{om,i} M_o} \tag{11}$$

In total the two-product model in ADCHEM considers 37 different surrogate oxidation products, of which 35 of them are surrogate compounds for the SOA oxidation products and 2 of them are surrogate compounds for the emitted POA (see table S2). The partitioning coefficient and mass

based stoichiometric yield of the two POA compounds were chosen so that the volatility should be comparable with what is used in the 2D-VBS (see Sect. 2.4.4).

Table S2. Parameters used to calculate temperature dependent aerosol yields for oxidation products of different organic compounds.

Org. comp.	**Ox. Agent**	α_1	α_2	$K_{om,1}$ ($m^3/\mu g$)	$K_{om,2}$ ($m^3/\mu g$)	ΔH_1 (kJ/mol)	ΔH_2 (kJ/mol)	$T_{ref,1}$ (K)	$T_{ref,2}$ (K)
α-pinene	OH	0.5[a]	-	0.02[a]	-	40[a]	-	320[a]	-
	O_3	0.08[a]	0.42[a]	0.5[a]	0.005[a]	100[a]	38[a]	310[a]	310[a]
	NO_3	0.1[a]	-	0.02[a]	-	40[a]	-	310[a]	-
β-pinene	OH	1.0[a]	-	0.02[a]	-	60[a]	-	310[a]	-
	O_3	0.03[a]	0.38[a]	0.5[a]	0.005[a]	100[a]	40[a]	310[a]	300[a]
	NO_3	1.0[b]	-	0.0163[b]	-	60[b]	-	~310[b]	-
Δ3-carene	OH	0.054[b]	0.517[b]	0.043[b]	0.0042[b]	100[c]	40[c]	~310[b]	~310[b]
	O_3	0.128[b]	0.068[b]	0.337[b]	0.0036[b]	100[c]	40[c]	~310[b]	~310[b]
	NO_3	0.743[b]	0.257[b]	0.0088[b]	0.0091[b]	80[c]	40[c]	~310[b]	~310[b]
D-limonene	OH	0.239[b]	0.363[b]	0.055[b]	0.0053[b]	100[c]	40[c]	~310[b]	~310[b]
	O_3	0.03[c]	0.38[c]	0.055[c]	0.0053[c]	40[c]	100[c]	~310[b]	~310[b]
	NO_3	1.0[c]	-	0.055[c]		80[c]	80[c]	~310[b]	~310[b]
Isoprene	OH	0.232[d]	0.0288[d]	0.00862[d]	1.62[d]	-	-	-	-
	O_3	0.232[d]	0.0288[d]	0.00862[d]	1.62[d]	-	-	-	-
	NO_3	0.232[d]	0.0288[d]	0.00862[d]	1.62[d]	-	-	-	-
Benzene	OH+NO	0.072[e]	0.888[e]	3.315[e]	0.0090[e]	40[c]	40[c]	300[c]	300[c]
	$OH+HO_2$	0.37[e]	-	-	-	-	-	-	-
Toluene	OH+ NO	0.095[a]	0.20[a]	0.5[a]	0.005[a]	40[a]	40[a]	300[a]	300[a]
	$OH+HO_2$	0.36[e]	-	-	-	-	-		
Xylene	OH+NO	0.044[a]	0.15[a]	0.5[a]	0.005[a]	60[a]	60[a]	300[a]	300[a]
	$OH+HO_2$	0.30[e]	-	-	-	-	-	-	-
POA	OH, O_3, NO_3	0.28[c]	0.72[c]	1.0[c]	0.01[c]	130[c]	100[c]	300[c]	300[c]

[a]Values from Svendby et al., 2008, [b]Values from Griffin et al., 1999, [c]Estimated values for this work, [d]Values from Henze and Seinfeld, 2006, [e]Values from Ng et al., 2007

Benzene, toluene and xylene first react with OH followed by either reaction with NO, forming products with a low and temperature dependent SOA-yield, or with HO_2, which gives products which has a high and temperature independent SOA-yield (at least for M_o>10μg/m^3) (Ng et al., 2007). In this study the two-product model SOA yields through the HO_2-pathway were assumed

to be constant also below 10µg/m^3 M_o, described by completely non-volatile oxidation products ($K_{om,i}=\infty$). At high NO_x/HO_2 ratio, which generally is the case in urban environments, most of the oxidation products will react with NO, while at remote regions the HO_2-pathway will dominate. Therefore, oxidation of benzene, toluene and xylene (BTX) in urban environments generally gives relatively low SOA formation, while moving further away from the source the SOA formation can be considerably higher. Here it is mainly benzene, which is the least reactive of the three compounds, that is left to form SOA (Henze et al., 2008). In ADCHEM both the high and low NO_x reaction pathways are considered simultaneously. The fraction reacting through the low-NO_x pathway is given by Eq. 12 from Ng et al. (2007). The reaction rate for the low-NO_x pathway is given by $k_{RO_2+HO_2} = 1.4 \cdot 10^{-12} \exp(700/T)$ cm^3 molecule^{-1} s^{-1} and the reaction rate for the high-NO_x pathway by $k_{RO_2+NO} = 2.6 \cdot 10^{-12} \exp(350/T)$ cm^3 molecule^{-1} s^{-1} (the Master Chemical Mechanism v 3.1 (http://www.chem.leeds.ac.uk/Atmospheric/MCM/mcmproj.html)).

$$f_{low-NO_x} = \frac{k_{RO_2+HO_2}[HO_2]}{k_{RO_2+NO}[NO] + k_{RO_2+HO_2}[HO_2]} \tag{12}$$

The heats of vaporization (ΔH) which gives the temperature dependence of the partitioning coefficients for the two-product model oxidation products from α-pinene, β-pinene, xylene and toluene were taken from Svendby et al. (2008). The temperature dependent partitioning coefficients are given by the Clausius Clapeyron relation (Eq. (13)) from e.g. Sheehan and Bowman (2001). The heats of vaporization (ΔH) of the two product model compounds formed from oxidation of benzene through the NO-pathway were assumed to be the same as for toluene.

$$K_{om}(T) = K_{om,ref} \frac{T}{T_{ref}} \exp\left[\frac{\Delta H}{R}\left(\frac{1}{T} - \frac{1}{T_{ref}}\right)\right] \tag{13}$$

2.4.2 Kinetic SOA formation with the 2D-VBS model

The 2D-VBS scheme used in ADCHEM classifies the organic compounds into 10 discrete volatility bins, separated by powers of 10 in C*, ranging from 10^{-2} to 10^{7} µg m^{-3} and 11 discrete O:C-ratios, separated by 0.1, from 0 to 1 (in total 110 (11x10) bins). The mass fraction F_i in the particle phase in each volatility bin i is given by Eq. (14) (Donahue et al., 2006).

$$F_i = (1 + C_i^* / M_o)^{-1} \tag{14}$$

For compounds with C* equal to 1 µg m^{-3}, Eq. (14) indicates that 50 % of these compounds will be found in the particle phase and 50 % in the gas phase, if the total particle organic mass content (M_o) is equal to 1 µg m^{-3}.

The temperature dependence of C* is given by Eq. (13) if K_{om} is replaced with C*. The heat of vaporization is calculated with a recently proposed expression (Eq. (15)) which states that the heat of vaporization can be estimated as a function of the saturation concentration (Epstein et al., 2010). C^*_{300} in Eq. (15) is the saturation concentration at 300 K.

$$\Delta H = -11 \cdot \log_{10} C^*_{300} + 129 \quad kJ\ mol^{-1} \qquad (15)$$

In the 2D-VBS model used in ADCHEM the traditional SOA precursors (BTX, monterpenes and isoprene) are first allowed to react according to their species specific reaction rates, and then all oxidation products are incorporated into the 2D-VBS. The volatility and O:C-ratio distribution of these first oxidation step reaction products were calculated with the functionalization and fragmentation algorithms used in the 2D-VBS model (see Sect. 2.4.3). The saturation concentrations and O:C-ratios of these primary oxidation products range between 10^7 and 10^1 µg m^{-3} and 0 and 0.4 respectively.

Jimenez et al. (2009) assumed that all organic compounds after the first oxidation step react with the OH radical with a gas-phase rate constant (k_{OH}) of $3 \cdot 10^{-11}$ cm^3 $molecules^{-1}$ s^{-1}, and state that the heterogeneous oxidation rate of organic compounds in the particle phase is at least 10 times slower. After one or a few oxidation reactions in the atmosphere the oxidation products lose their original signature and become increasingly similar in structure independent of the original molecular structure (Jimenez et al., 2009). Therefore, for all gas phase compounds in the 2D-VBS, the same k_{OH} of $3 \cdot 10^{-11}$ cm^3 $molecules^{-1}$ s^{-1} as proposed by Jimenez et al. (2009) was also used in ADCHEM. All gas phase compounds in each 2D-VBS bin were also assumed to be oxidized by O_3 and NO_3 with $k_{O3}=10^{-17}$ cm^3 $molecules^{-1}$ s^{-1} and $k_{NO3}=10^{-14}$ cm^3 $molecules^{-1}$ s^{-1}, which are approximately the reaction rates for alkenes (Atkinson, 1997). The heterogeneous reactions were assumed to be insignificant compared to the gas phase, and were therefore neglected.

2.4.3 Functionalization and fragmentation of organic oxidation products

Functionalization is the process by which oxidation reactions create new products with the same carbon number and higher O:C-ratio, while fragmentation creates products with lower carbon number and higher O:C-ratio. In ADCHEM the functionalization algorithm was adapted from Jimenez et al., 2009. In the algorithm it is assumed that all functionalization reactions, are independent of the properties of the organic reactant, the formed products take-up one to three oxygen atoms, where on molar basis 29 % take-up one oxygen atom, 49 % two oxygen atoms and 22 % three oxygen atoms. Since these oxygen atoms can attach differently to the carbon chain of the original molecule, there are also separate probability functions for the change in volatility (change of C* (ΔC*)) of the products which take-up one, two or three oxygen atoms, varying from -10^1 to -10^7 µg/m^3 (see Table. 1). The change in O:C-ratio upon functionalization depends on the number of carbon atoms of the original molecule. In the 2D-VBS the number of carbon atoms of the surrogate compounds varies between 29 for the bin (C*=10^{-2} µg/m^3, O:C-ratio=0) down to 2.3 for the bin (C*=10^7 bin µg/m^3, O:C-ratio=1). In the 2D-VBS an increase in C* by 10 without changing the O:C-ratio is achieved by removing 2 carbon atoms from a compound, while an addition of one oxygen molecule decreases the saturation concentration 3.75 times more than if hypothetically one carbon atom was added. These values are in fair agreement with the values given in Pankow and Asher, 2008, which estimate that 2 extra carbon atoms increases the vapor pressure by almost 10 and depending on whether the oxygen atoms form hydroxyl-, aldehyde-, ketone or carboxylic acid- groups the vapor pressure decreases with 2-5 times more than if just adding one carbon atom.

Table 1. Probability functions for the change in C* when adding one to three oxygen atoms (O) to the organic compounds in the 2D-VBS.

ΔC* (µg/m^3)	-10^1	-10^2	-10^3	-10^4	-10^{-5}	-10^6	-10^7
+1 O	0.30	0.50	0.20				
+2 O		0.19	0.38	0.32	0.11		
+3 O			0.095	0.20	0.41	0.20	0.095

In the 2D-VBS used in ADCHEM all oxidation reactions first follows the functionalization kernel and then a fraction (*f*) of the formed oxidation products will fragmentize. Equivalent to Jimenez et al. (2009) it is assumed that the molecules that fragmentize have equal probability to split at any of the carbon bonds. For C11 molecules which fragmentize there will in average, on molar basis, be 10 % of all C1 to C10 molecules. Each of the 2D-VBS bins on the right side of

the original molecule (higher C*) bin will therefore receive the same number of molecules, but different masses. Jimenez et al. (2009) assumed that part of the formed fragments have unchanged O:C-ratio while others increases their O:C-ratio. However, in the 2D-VBS used in ADCHEM it is simply assumed that the fragments from the oxidation products (formed from the functionalization reactions) always have the same O:C-ratio as the non-fragmentized molecule. Since the fragments first take-up oxygen atoms before they fragmentize, they still always have larger O:C-ratio than the original molecule (before reaction).

One large uncertainty with the VBS model approach is how to estimate the fraction (*f*) of the oxidation reactions which cause the organic molecules to fragmentize (form products with lower carbon number and higher O:C-ratio) and which fraction that functionalizes (form new products with the same carbon number and higher O:C-ratio). Jimenez et al. (2009) proposed that the fraction of reactions that cause fragmentation at low NO_x conditions can be given as a function of the O:C-ratio according to Eq. (15). This equation is also used in the 2D-VBS model in ADCHEM, both for low and high NO_x conditions. The different benzene, toluene and xylene SOA yields between the low and high NO_x conditions are instead assumed to be caused by the first oxidation reactions before these compounds enter the 2D-VBS. To account for the different yields, the benzene, toluene and xylene molecules reacting through the high NO_x pathway are always assumed to be fragmentized when they are oxidized, while those reacting through the low NO_x pathway are always functionalized. The monoterpenes and isoprene are always assumed to react through the low NO_x pathway, independent of the NO and HO_2 concentration. Figure S1 in the supplementary material compares the modeled yields with the 2-product model parameterization of the measured BTX yields from Ng et al. (2007). For atmospheric relevant particle organic mass concentrations (1-10 μg/m^3) the yield for BTX with the 2D-VBS is about 4-11 % for high NO_x conditions, while 15-35 % for low NO_x conditions, at 300 K. This can be compared with the 2-product model SOA yields of 5-15 % for benzene, 2-8 % for toluene and 1-4 % for xylene at high NO_x conditions and 37 % for benzene, 36 % for toluene and 30 % for xylene at low NO_x conditions.

$$f = \left(\frac{O}{C}\right)^{1/6} \qquad (15)$$

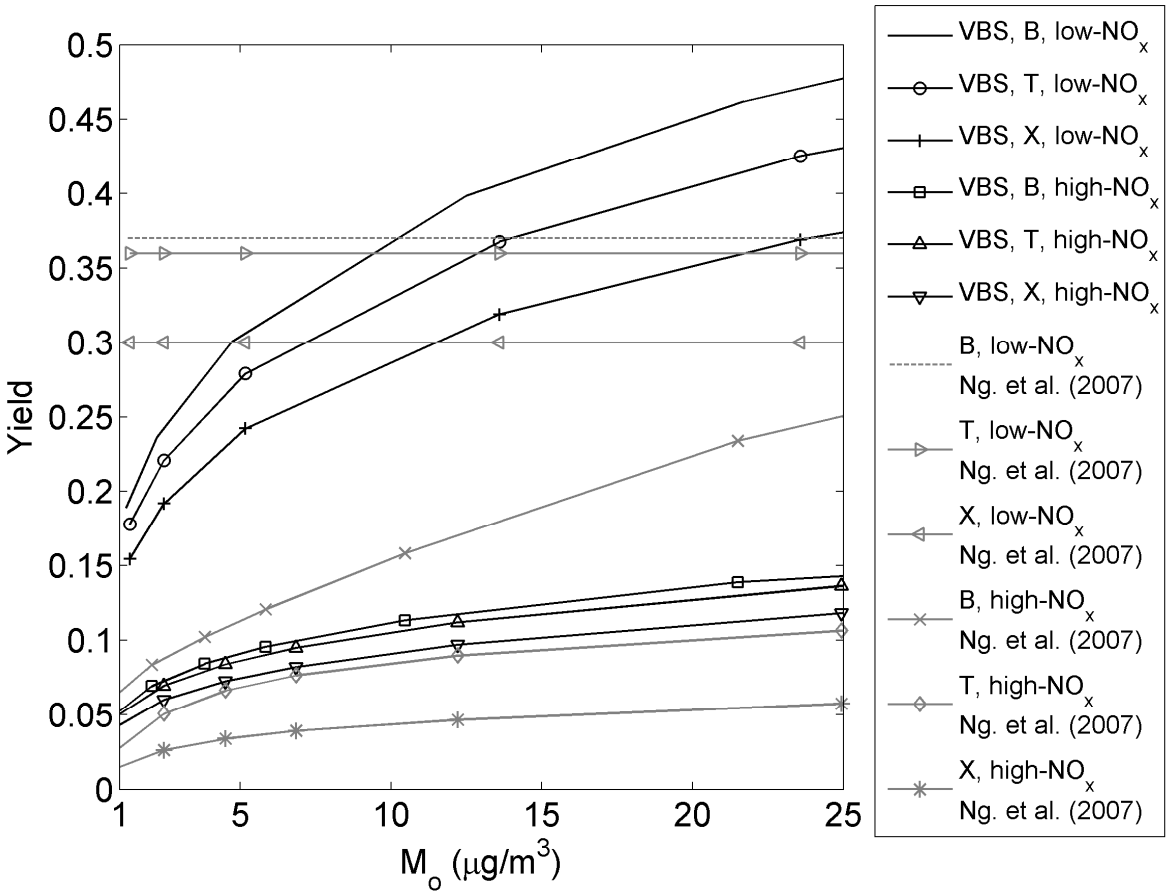

Figure S1. SOA Yield for benzene (B), toluene (T) and xylene (X), at 300 K, at high NO_x and low NO_x conditions (Ng et al., 2007) and benzene, toluene and xylene SOA yield at 300 K from 2D-VBS model used in ADCHEM.

2.4.4 POA volatility

Another key uncertainty in the modeled organic aerosol formation in urban environments is the volatility of the organic emissions traditionally considered to be POA (e.g. Shrivastava et al., 2008 and Tsimpidi et al., 2010). Shrivastava et al. (2008) used the 3D-CTM model PMCAMx to model the organic aerosol in the US by either treating these traditional POA emissions as non-volatile (C*=0) or as semi-volatile (C* between 10^{-2} and 10^{4} μg m^{-3}). Their results illustrate that condensation of oxidized organic compounds formed from compounds which first evaporates after dilution and then are oxidized in the atmosphere has the potential to significantly increase the summertime organic aerosol (OA) in urban environments in the USA. In this work the traditional POA emissions (e.g. from EMEP) was either treated as non-volatile compounds (C*=0 μg m^{-3}) or as semi-volatile. These semi-volatile POA

(SVPOA) mass emissions were divided into different C* channels according to the work by Robinson et al. (2007), Shrivastava et al. (2008) and Tsimpidi et al. (2010). Analogous with Robinson et al. (2007), Shrivastava et al. (2008) and Tsimpidi et al. (2010) the intermediate volatile organic carbon (IVOC) emissions (C* between 10^4 and 10^6 $\mu g\ m^{-3}$), was assumed to be proportional and 1.5 times larger than the POA emissions (see Table S3 in the online supplementary material).

Table S3. Emission fractions of existing non-volatile POA emissions if treating the POA as semi-volatile and including IVOC emissions.

C* at 298 K ($\mu g/m^3$)	10^{-2}	10^{-1}	1	10^1	10^2	10^3	10^4	10^5	10^6
Emission fractions[a] SVPOA	0.03	0.06	0.09	0.14	0.18	0.30	0.20	0	0
Emission fractions[a] IVOCs	0	0	0	0	0	0	0.20	0.50	0.80

[a]Mass ratio to existing EMEP POA emissions, values adopted from Robinson et al. (2007), Shrivastava et al. (2008) and Tsimpidi et al. (2010).

Recently performed chamber measurements on wood smoke and diesel car POA emissions indicate that the POA may evaporate slowly before reaching an equilibrium with the gas phase (at least 1 hour) (Grieshop et al., 2009). The spatial and temporal resolution used in ADCHEM enables the treatment of this mass transfer limited evaporation. Therefore all POA emissions in ADCHEM are initially placed in the particle phase, although they at equilibrium to a large fraction will be found in the gas phase. This enables ADCHEM to study the kinetic evaporation of the SVPOA downwind the source region, followed by the oxidation of the SVPOA in the gas phase and finally the re-condensation of the oxidized SVPOA several hours after the initial emissions.

References

Atkinson. R. Gas-phase tropospheric chemistry of volatile organic compounds .1. Alkanes and alkenes. Journal of physical and chemical reference data 26, 215-290, 1997.

Donahue, N. M., Robinson, A. L., Stanier, C. O., Pandis, S. N. Coupled partitioning, dilution, and chemical aging of semivolatile organics.
Environmental Science and Technology 40, 2635–2643, 2006.

Epstein S., Riipinen I. and Donahue N. M. A Semiempirical Correlation between Enthalpy of Vaporization and Saturation Concentration for Organic Aerosol. Environ. Sci. Technol., 44, 743–748, 2010.

Grieshop A. P, Miracolo M. A., Donahue N. M. and Robinson A. L. Constraning the Volatility Distribution and Gas-Particle Partitioning of Combustion Aerosols Using Isothermal Dilution and Thermodenuder Measurements. Environ. Sci. Technol. 43, 4750-4756.

Griffin R. J., Cocker III D. R., Flagan R. C., Seinfeld J. H. Organic aerosol formation from the oxidation of biogenic hydrocarbons. J. Geophys. Res., 107, D3, 3555-3567, 1999.

Henze D. K. and Seinfeld J. H. Global secondary organic aerosol from isoprene oxidation. Geophysical Research Letters, 33 L09812, 2006.

Henze D. K., Seinfeld J. H., Ng N. L., Kroll J. H., Fu T.-M., Jacob D. J., Heald C. L. Global modeling of secondary organic aerosol formation from aromatic hydrocarbons: high- vs. low-yield pathways. Atmos. Chem. Phys., 8, 2405-2421, 2008.

Jacobson M. Z. Numerical techniques to solve condensational and dissolutional growth equations when growth is coupled to reversible aqueous reactions. Aerosol Sci. Technol. 27, 491-498, 1997.

Jacobson M. Z. A Solution to the Problem of Nonequilibrium Acid/Base Gas-Particle Transfer at Long Time Step. Aerosol Science and Technology, 39, 92-103, 2005a.

Jimenez J. L., Canagaratna M. R., Donahue N. M., Prevot A. S. H., Zhang Q., Kroll J. H., DeCarlo P. F., Allan J. D., Coe H., Ng N. L., Aiken A. C., Docherty K. S., Ulbrich I. M., Grieshop A. P., Robinson A. L., Duplissy J., Smith J. D., Wilson K. R., Lanz V. A., Hueglin C., Sun Y. L., Tian J., Laaksonen A., Raatikainen T., Rautiainen J., Vaattovaara P., Ehn M., Kulmala M., Tomlinson J. M., Collins D. R., Cubison M. J., Dunlea E. J., Huffman J. A., Onasch T. B., Alfarra M. R., Williams P. I., Bower K., Kondo Y., Schneider J., Drewnick F., Borrmann S., Weimer S., Demerjian K., Salcedo D., Cottrell L., Griffin R., Takami A., Miyoshi T., Hatakeyama S., Shimono A., Sun J. Y, Zhang Y. M., Dzepina K., Kimmel J. R., Sueper D., Jayne J. T., Herndon S. C., Trimborn A. M., Williams L. R., Wood E. C., Middlebrook A. M., Kolb C. E., Baltensperger U., Worsnop D. R., Evolution of Organic Aerosols in the Atmosphere. Science 326, 1525-1529, 2009.

Korhonen H. Model studies on the size distribution dynamics of atmospheric aerosols. Report series in aerosol science, No 65. Finnish association for aerosol research. ISBN: 952-5027-46-5, 2004a.

Ng N.L., Kroll J. H., Chan A. W. H., Chhabra P. S., Flagan R. C. and Seinfeld J. H. Secondary organic aerosol formation from m-xylene, toluene, and benzene. Atmospheric Chemistry and Physics, 7, 3909-3922, 2007.

Odum J. R., Hoffmann T., Bowman F., Collins D., Flagan R. C. And Seinfeld J. H. Gas/Particle Partitioning and Secondary Organic Aerosol Yields. Environ. Sci. Technol., 30, 2580-2585, 1996.

Pankow J. F. An absorption model of the gas/aerosol partitioning involved in the formation of secondary organic aerosol. Atmospheric Environment, 28, 189-193, 1994.

Pankow J. F. and Asher W. E.. SIMPOL.1: a simple group contribution method for predicting vapor pressures and enthalpies of vaporization of multifunctional organic compounds. Atmos. Chem. Phys., 8, 2773–2796, 2008.

Pirjola L. and Kulmala M. Modelling the formation of H_2SO_4-H_2O particles in rural, urban and marine conditions. Atmos. Res., 46, 321-347, 1998.

Robinson A. L., Donahue N. M., Shrivastava M. K., Weitkamp E. A., Sage A. M., Grieshop A. P., Lane T. E., Pierce J. R., Pandis S. N. Rethinking organic aerosols: Semivolatile emissions and photochemical aging. Science, 315, 1259-1262, 2007.

Roldin P. , Swietlicki E. , Massling A., Kristensson A., Löndahl, J., Eriksson A., Pagels J. and Gustafsson S. Aerosol ageing in an urban plume - Implications for climate and health. Submitted to Atmospheric Chemistry and Physics Discussion, 2010.

Sander S. P., Friedl R. R., Golden D. M., Kurylo M. J., Moortgat G. K., Keller-Rudek H., Wine P. H., Ravishankara A. R., Kolb C. E., Molina M. J., Finlayson-Pitts B. J., R. E. Huie and Orkin V. L. Chemical Kinetics and Photochemical Data for Use in Atmospheric Studies. Evaluation Number 15. NASA, 2006

Sheehan P. E. and Bowman F. M. Estimated Effects of Temperature on Secondary Organic Aerosol concentrations. Environmental Science and Technology, 35, 2129-2135, 2001.

Shrivastava M. K., Lane T. E., Donahue N. M., Pandis S. N. and Robinson A. L. Effects of gas particle partitioning and aging of primary emissions on urban and regional organic aerosol concentrations. Journal of Geophysical Research, 113, D18301, doi:10.1029/2007JD009735, 2008.

Svendby T. M., Lazaridis M. and Tørseth K. Temperature dependent secondary organic aerosol formation from terpenes and aromatics. Journal of Atmospheric Chemistry, 59, 25-46, 2008.

Tsimpidi A. P., Karydis V. A., Zavala M., Lei W., Molina L., Ulbrich I. M., Jimenez J. L. and Pandis S. N. Evaluation of the volatility basis-set approach for the simulation of organic aerosol formation in the Mexico City metropolitan area. Atmos. Chem. Phys., 10, 525–546, 2010.

Wexler A. S. and Seinfeld J. H. The distribution of ammonium salts among a size and composition dispersed aerosol. Atmospheric Environment 24, 1231–1246, 1990.

Zaveri R. A., Easter R. C., Fast J. D. and Peters L. K. Model for Simulating Aerosol Interactions and Chemistry (MOSAIC). Journal of Geophysical Research, 113, D13204, doi:10.1029/2007JD008782, 2008.

Zhang K. M. and Wexler A. S. Modeling urban and regional aerosols-Development of the UCD Aerosol Module and implementation in CMAQ model. Atmospheric Environment, 42, 3166-3178, 2008.